Received: 28 April 2021 | Revised: 23 August 2021 | Accepted: 29 August 2021

DOI: 10.1111/jzs.12537

SPECIAL ISSUE

JOURNAL OF ZOOLOGICAL SYSTEMATICS AND EVOLUTIONARY RESEARCH

WILEY

First insights into the origin of Iranian cave beetle diversity with description of two new species of the genus *Duvalius* (Carabidae)

Mohammad Javad Malek-Hosseini[1,2,3] | **Jan Muilwijk**[4] | **Matjaž Gregorič**[2] | **Matjaž Kuntner**[1,2] | **Klemen Čandek**[1]

[1]Department of Organisms and Ecosystems Research, National Institute of Biology, Ljubljana, Slovenia

[2]Jovan Hadži Institute of Biology, Research Centre of the Slovenian Academy of Sciences and Arts, Ljubljana, Slovenia

[3]Department of Biology, Biotechnical Faculty, University of Ljubljana, Ljubljana, Slovenia

[4]Department of Entomology, Naturalis Biodiversity Centre, Leiden, The Netherlands

Correspondence
Mohammad Javad Malek-Hosseini, Department of Organisms and Ecosystems Research, National Institute of Biology, Ljubljana, Slovenia; Jovan Hadži Institute of Biology, Research Centre of the Slovenian Academy of Sciences and Arts, Ljubljana, Slovenia; Department of Biology, Biotechnical Faculty, University of Ljubljana, Ljubljana, Slovenia.
Email: Malekhosseini1365@gmail.com

Jan Muilwijk, Department of Entomology, Naturalis Biodiversity Centre, Darwinweg 2, 2333 CR Leiden, The Netherlands.
Email: Jan.Muilwijk@gmail.com

Funding information
Biotechnical Faculty of the University of Ljubljana; Uyttenboogaart-Eliasen Stichting, Grant/Award Number: 2017.12.03; Slovenian Research Agency, Grant/Award Number: P1- 0236, P1-0255, J1-9163 and J1-1703

Abstract

Subterranean environments of Iran are severely understudied. Here, we advance the knowledge of Iranian cave biodiversity by following three goals: (i) to investigate Iranian caves for troglobiotic beetles; (ii) to understand the phylogenetic relationships and estimate the timing of Iranian cave colonization by *Duvalius* Delarouzée, 1859; and (iii) to comment on the current knowledge of the Iranian troglobiotic fauna to facilitate future research. Through field efforts and morphological examination, we describe two new *Duvalius* species from caves of Zagros Mts., Iran: the troglobiotic *Duvalius nezelensis* sp. nov. and the non-troglobiotic *Duvalius achaemenius* sp. nov. For phylogenetic analyses, we provide original sequences of two mitochondrial (*COI*, *16S*) and two nuclear (*18S*, *28S*) genes for three *Duvalius* species from the Zagros Mts., and combine them with published molecular datasets using other *Duvalius* species with relevant outgroup genera. Using Bayesian inference and maximum likelihood, we reconstruct a species-level phylogeny of *Duvalius* and closely related genera, then use BEAST to explore divergence times of major lineages. Our phylogenies recover a well-supported "Zagros clade," with its split from other congeners estimated at 9.7 Ma. Within the Zagros clade, the split of *D. nezelensis* and its sister group is estimated at 7.8 Ma, while the split of *D. achaemenius* and *D. kileri* is estimated to a recent 0.78 Ma. We provide some resolution in understanding the species richness of cave beetles in Iran and the timing of their subterranean colonization. However, our phylogenies confirm taxonomic problems as several genera are nested deep within the *Duvalius* tree.

KEYWORDS
Duvalius, molecular phylogeny, Trechini, troglobiont, Zagros

Résumé

Les environnements souterrains de l'Iran sont très peu étudiés. Dans le présent article nous améliorons les connaissances sur la biodiversité des grottes iraniennes en suivant trois objectifs : (i) étudier les grottes iraniennes à la recherche de coléoptères

Contributing authors: Matjaž Gregorič (matjaz.gregoric@zrc-sazu.si), Matjaž Kuntner (Matjaz.Kuntner@nib.si), Klemen Čandek (klemen.candek@nib.si)

Zoobank links: LSID: http://zoobank.org/urn:lsid:zoobank.org:act:53D2B6C8-8496-4B36-B2D3-A518FC4EE287 **Online ISSN**: 1439-0469

LSID: http://zoobank.org/urn:lsid:zoobank.org:act:1F57B27C-43F8-40EA-B4D9-082E7F334BDF

troglobies ; (ii) comprendre les relations phylogénétiques et estimer la date de colonisation des grottes iraniennes par le genre *Duvalius* Delarouzée, 1859 ; et (iii) commenter les connaissances actuelles de la faune troglobie iranienne afin de faciliter les recherches futures. Par du travail de terrain et un examen morphologique, nous décrivons deux nouvelles espèces de *Duvalius* provenant de grottes des monts Zagros, en Iran : la troglobie *Duvalius nezelensis* sp. nov. et la non-troglobie *Duvalius achaemenius* sp. nov. Pour les analyses phylogénétiques, nous fournissons les séquences originales de deux gènes mitochondriaux (*COI*, *16S*) et de deux gènes nucléaires (*18S*, *28S*) pour trois espèces de *Duvalius* des monts Zagros, et nous les combinons avec des données moléculaires publiés sur d'autres espèces de *Duvalius* et sur des groupes externes pertinents. En utilisant l'inférence bayésienne et le maximum de vraisemblance, nous reconstruisons une phylogénie au niveau des espèces de *Duvalius* et des genres qui leur sont étroitement apparentés, puis nous utilisons BEAST pour explorer les temps de divergence des principales lignées. Nos phylogénies révèlent un “clade Zagros” bien étayé, dont la séparation avec ses congénères est estimée à 9,7 Ma. Au sein du clade Zagros, la séparation de *D. nezelensis* et de son groupe frère est estimée à 7,8 Ma, tandis que la séparation de *D. achaemenius* et *D. kileri* est estimée à une date récente de 0,78 Ma. Nous apportons une certaine résolution dans la compréhension de la richesse en espèces des coléoptères des cavernes en Iran et de la chronologie de leur colonisation du milieu souterrain. Cependant, nos phylogénies confirment des problèmes taxonomiques, car plusieurs genres sont imbriqués profondément dans l'arbre du genre *Duvalius*.

1 | INTRODUCTION

Globally, subterranean environments have been colonized by several groups of animals, for example, fishes, amphibians, molluscs, and many arthropod groups (Vandel, 1964). Iran has some of the largest cave systems in the world (Raeisi et al., 2012; Vatandoust et al., 2019), yet most of them are poorly investigated. Troglobiotic representatives of fishes, millipedes, spiders, crustaceans, and snails are already recorded from Iranian caves (Bargrizaneh et al., 2021; Fatemi et al., 2019; Malek-Hosseini & Zamani, 2017). However, even though beetles are among the arthropod groups with globally species-richest terrestrial troglobiotic representatives (Zagmajster et al., 2008), only a single true cave-dwelling beetle, *Foranotum perforatum* Nabozhenko & Sadeghi, 2017 (Tenebrionidae), is known from Iran (Nabozhenko & Sadeghi, 2017). Troglophile and trogloxene representatives of several beetle families occur in Iran, including the genera *Laemostenus* and *Duvalius* (Carabidae) from caves in the Zagros and Central zone (Tahami et al., 2017). All Iranian *Duvalius* are recorded almost exclusively from the Zagros Mountains (Malek-Hosseini et al., 2016), an extensive, 1500 km mountain range from north-west to south Iran. These mountains have a sedimentary origin being composed primarily of limestone. Geologically, Zagros is part of the Alpine-Himalayan orogenic belt (Agard et al., 2011; Cucchi & Zini, 2003).

With around 300 species, the genus *Duvalius* Delarouzée, 1859 is one of the most species-rich genera of the family Carabidae. Most *Duvalius* species are West Palaearctic elements, but some are found in West China, Kyrgyzstan, Caucasus, Armenia, Pakistan, Afghanistan, Turkmenistan, and most species have restricted distributions (Belousov, 2017). *Duvalius* belongs to the tribe Trechini, which is one of the main insect groups that have colonized subterranean environments (Faille et al., 2011). Comprising numerous true cavernicolous species, trechine ground beetles of West Palaearctic are well studied morphologically, yet the evolutionary origins of some groups of these beetles are enigmatic due to incomplete sampling (Faille et al., 2013; Maddison et al., 2019). Trechini includes over 2500 species distributed worldwide (Bousquet, 2012), originated in Eocene to early Oligocene, and comprise numerous lineages that have colonized the subterranean world (Maddison et al., 2019). *Duvalius* is one of the Trechini lineages (“isotopic” Trechini), which has probably rapidly diversified during late Miocene (Faille et al., 2013). However, the genus level taxonomy is unresolved: While the *Duvalius* lineage is reported to include no fewer than eight genera (*Anophthalmus*, *Arctaphaenops*, *Agostinia*, *Duvalius* sensu stricto, *Luraphaenops*, *Trichaphaenops*, *Aphaenopidius*, and *Petraphaenops*), the relationships among these genera, and even their monophyly, remain ambiguous (Delić et al., 2020; Faille et al., 2013).

Species described as *Duvalius* s.s. are found in different ecological environments, and the cavernicolous ones show different degrees of troglomorphism. These species show slight or complete depigmentation, and reduced or absent eyes and wings, while other species are pigmented and even winged (albeit exceptionally; Deuve, 2000; Faille et al., 2013). To date, four species of *Duvalius* have been

known from Iran, of which three are endemic to Zagros Mts., and *D. hetschkoi* (Reitter, 1911) with a wide distribution area. The apterous nominate form of *D. hetschkoi* (Reitter, 1911) is described from Turkmenistan and also occurs in Afghanistan, and *D. hetschkoi orbayi* Hernando, 1999 is known from Pakistan (Belousov, 2017; Deuve, 2000). The Iranian subspecies *D. hetschkoi matilei* Deuve, 2000 is the only known *Duvalius* with the exceptional feature of having functional wings. *D. hetschkoi*, including its subspecies, has an exceptionally large and disjointed distribution range (Belousov, 2017; Deuve, 2000). In the prominent monograph by Jeannel (1928), *D. hetschkoi* is placed together with *D. bodoanus* (Reitter, 1913) and *D. dromioides* (Reitter, 1897) in the "*bodoanus*" species group. Later Kryzhanovskij et al. (1995) assumed that *D. dromioides* (Reitter, 1897) should be placed in the genus *Oroblemites* (Ueno & Pawlowski, 1981). Jeannel based the similarity of the species of the "*bodoanus*" species group on the big eyes and stated that these species possess the same type of bifid copulatory piece in the median lobe as species from central Caucasus, Greece, and Italy.

The other Iranian species are restricted to the Central and Southern parts of the Zagros Mts.: *Duvalius koeni* Muilwijk & Felix, 2008, *Duvalius mohammadzadehi* Muilwijk & Felix, 2008 (Muilwijk & Felix, 2008), and *Duvalius kileri* Muilwijk & Malek Hosseini 2016 (Malek-Hosseini et al., 2016). These species are similar to *D. hetschkoi* and form the *hetschkoi* species group. Other *Duvalius* species occur in the neighboring countries of Iran.

D. antoniae (Reitter, 1892) has been recorded from the border area between Armenia and Azerbaijan (Mount Ilandag, North of Ordubad). This species is very close to *D. stepanavanensis* Iablokoff-Khnzorian 1963. Also, two species from East Turkey are close to this group *D. martinae* Jeanne 1996 and *D. armeniacus* Casale, 1979. This Armenian species group is recognizable by its tibiae without external sulcus, its chaetotaxy, lack of eyes, and morphology of the copulatory apparatus (Casale, 1979) and therefore differs from the *hetschkoi* species group (Jeannel, 1928).

Here, we investigate the subterranean beetle fauna of Iranian caves of the Zagros Mts. We diagnose and describe two newly discovered species of *Duvalius* Delarouzée, 1859 from two caves in Zagros. The troglobiotic *Duvalius nezelensis* sp. nov. occurs in the Nezel cave, while the troglophile *Duvalius achaemenius* sp. nov. occurs in the small Suq cave. We then use molecular phylogenetic analyses to include the new species in a phylogenetic framework. Specifically, we aim to obtain a dated phylogeny that will enable understanding of the timing of cave colonization by beetles in the region. Finally, we use the newly presented data to provide preliminary interpretations of the troglobiotic Iranian fauna species richness.

2 | METHODS

2.1 | Taxon sampling

We obtained original, four marker sequences (see below) of three *Duvalius* species from the Zagros Mts., Iran: *D. achaemenius* sp. nov., *D. kileri*, and *D. nezelensis* sp. nov. For morphological examination and measurements, we used five specimens of *D. achaemenius*, seven specimens of *D. kileri* (one specimen was previously published in Malek-Hosseini et al., 2016), and eight specimens of *D. nezelensis*, of which we used one specimen per species for DNA isolation. The

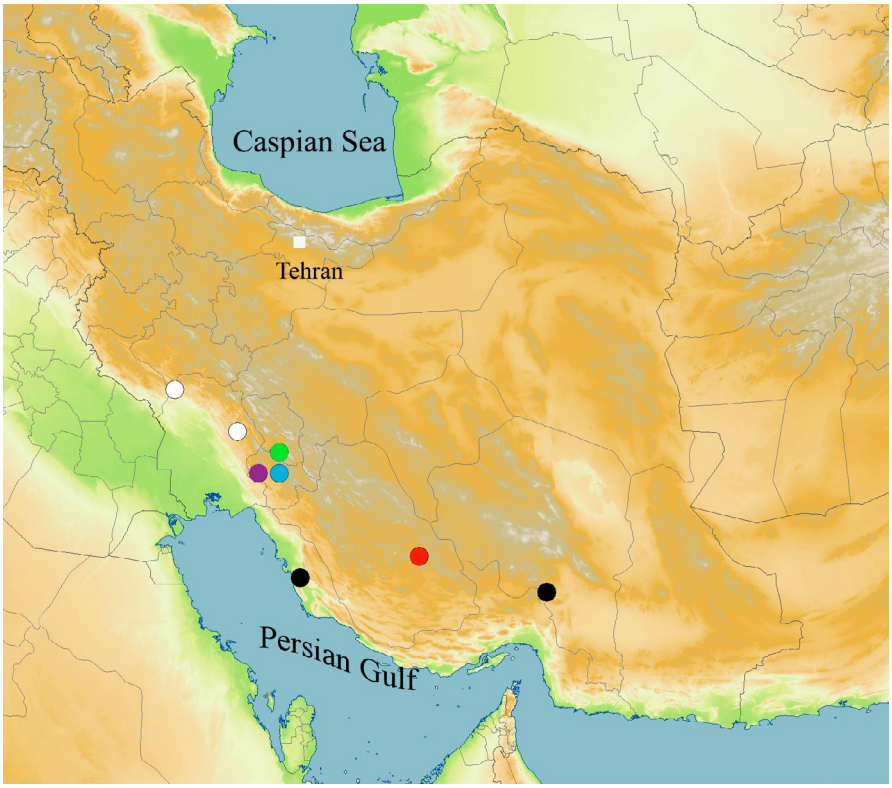

FIGURE 1 Location of investigated caves in Iran and distribution of Iranian *Duvalius*. Purple circle: *Duvalius (D.) achaemenius* sp. nov. Black circles: *Duvalius (D.) hetschkoi matilei* Deuve, 2000. Green circle: *Duvalius (D.) kileri* Muilwijk & Malek Hosseini, 2016. White circles: *Duvalius (D.) koeni* Muilwijk & Felix, 2008. Orange circle: *Duvalius (D.) mohammadzadehi* Muilwijk & Felix, 2008. Blue circle: *Duvalius (Duvalius) nezelensis* sp. nov

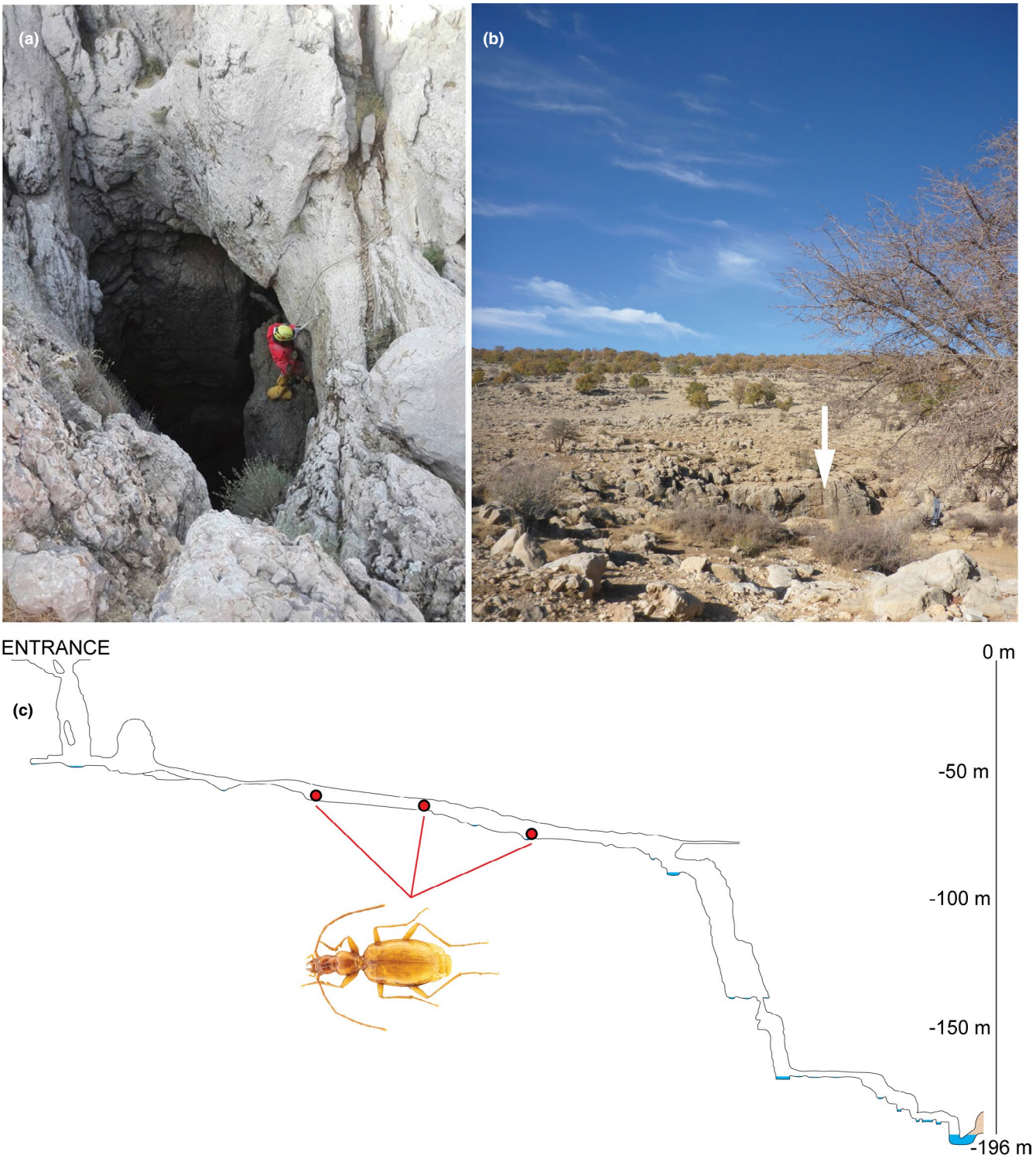

FIGURE 2 Nezel cave: (a) The entrance of the cave that is a 50-m pit. (b) The same entrance of the cave as figure 2a from another view that is located in a flat plain (white arrow showing the entrance). (c) Sampling localities within the Nezel cave (red circles showing the places where specimens of *Duvalius nezelensis* sp. nov. were found)

Iranian *Duvalius* species *D. koeni* (two specimens, previously published in Muilwijk & Felix, 2008), *D. mohammadzadehi* (two specimens, previously published in Muilwijk & Felix, 2008), and *D. hetschkoi matilei* (one specimen, previously published in Deuve, 2000) were used for morphological comparison with the above three species (Appendix 1). From GenBank, we additionally mined the same four marker sequences for nine genera that are hypothesized to be nested within the *Duvalius* clade (Delić et al., 2020; Faille et al., 2013): In total, we selected sequences of 43 species of *Duvalius*, 11 species of *Anophthalmus*, and for representatives of *Agostina* (1), *Aphaenopidius* (2), *Arctaphaenops* (1), *Luraphaenops* (1), *Petraphaenops* (1), and *Trichaphaenops* (1) (Table S3). *Pheggomisetes globiceps* Buresch, 1925,

Geotrechus discontignyi (Fairmaire, 1867), *Aphaenops cereberus* (Dieck, 1869), and *A. leschenaulti* Bonvouloir, 1862 were used as outgroups.

2.2 | Field work and cave details

During several expeditions to Nezel and Suq caves, both in the Kohgiluyeh Va Boyer Ahmad Province in the Central part of the Zagros Mountains, South-Western Iran (Figure 1) between 2015 and 2019, the first and second authors collected the material by hand.

The Nezel cave is a natural cave in Southwest Iran near Jookhooneh Village, Kohgiluyeh Va Boyer Ahmad Province (30°47′28.62″ N, 50°56′53.83″ E, altitude 2307 m above sea level (a.s.l.), depth of the cave: −196 m, length of discovered part is 546 m). The entrance of the cave is a 50-meter pit, located in a flat plain (Figure 2). The cave consists of several pits of different depths, the last pits are siphons, and the total depth is 196 m ending in a siphon. The cave contains two big halls. During heavy rain, streams of water flow through the first hall. The second hall includes a big water pool with almost no mud. Environmental conditions at the collection site were as follows: water temperature: 8.6°C; pH: 7.8–8.3; air temperature: 10–11°C; CO_2: 388–1493 ppm; and relative humidity: 86–95%.

The Zagros Mts. chain represents the southern, Asian branch of the Alpine geosynclines. The Nezel cave is located on the Sarvak Formation in the Zagros Mountains. The age of this formation is determined as the Cenomanian (100–93 Ma) in most parts (Jamalpour et al., 2017; Parnian et al., 2019; Razin et al., 2010; Setudehnia, 1973). Orogeny and then speleogenesis could have occurred during Miocene (Popov et al., 2004). Nezel is still an active cave.

The Suq cave is a small natural cave in Southwest Iran, Kohgiluyeh Va Boyer Ahmad Province near Suq and Lendeh (30°49′25.9″ N, 50°25′37.9″ E, altitude 812 m a.s.l.). In the summer, the region is hot and dry, with temperatures exceeding 40°C. The cave is located in a gorge where a small brook flows through, with the opening at the level of the brook. The passable part of the cave is approximately 100 m long, with water flowing between small rocks. There is hardly any debris or mud between the stones. At the far end of the cave streams a larger brook.

2.3 | Morphological examination and imaging

Specimens were examined with a Leica MZ 20.5 C stereomicroscope. Genitalia were extracted after soaking of the specimen for at least 24 h in a commercial protein enzyme solution. Male genitalia were immersed in a water/alcohol mixture in several stages and preserved in Euparal. Measurements were mostly conducted from photographs. For measurements of the median lobe, a 10× Nikon microscope objective was used. Measurement of the length of median lobe was obtained with a microscope objective micrometer (0.01 mm). The median lobe length was measured from basal bulb to apex of apical lamella at the widest distance. Microsculpture was studied at 120× magnification. The elytral chaetotaxy is seen as black spots on the left elytron (Figures 3 and 4).

Photographs of beetles were taken with a Canon 5Ds digital camera and Canon MP-E 65 mm macro lens or a Nikon 10× objective, and subsequently stacked using Helicon Focus 7. The label text of type specimens or of historical specimens is cited as originally given, a forward slash (/) indicates the end of each line. A double forward slash (//) separates labels. All measurements are reported in millimeters.

The following morphological acronyms are used:

TL: total length measured from the anterior margin of labrum to the apex of elytra;
EL: elytral length measured along suture from the basal bead of the elytron to the apex;
EW: maximum width of the elytra;
PL: pronotal length measured along the middle line;
PW: maximum width of the pronotum.

The following museum and collection acronyms are used:

CMU: Working collection of Jan Muilwijk, Leiden, Netherlands;
HMIM: Hayk Mirzayan's Insect Museum, Tehran, Iran;
MNP: Národní Muzeum Praha, Czech Republic;
NBCL: Naturalis Biodiversity Centre, Leiden, Netherlands;
ZM–CBSU: Zoological Museum and Biological Collection of Shiraz University, Shiraz, Iran.

2.4 | Molecular procedures

One leg of a specimen from each species was taken for DNA extraction. The protocol included Robotic DNA extraction using Mag MAX™ Express magnetic particle processor Type 700 with DNA Multisample kit (Thermo Fisher Scientific kit) and modified protocols following Vidergar et al. (2014). We amplified fragments of four genes, two mitochondrial and two nuclear. Mitochondrial markers: 3′ end of cytochrome *c* oxidase subunit 1 gene (*COI*); a section including the 3′ end of the *16S rRNA* gene, the *tRNA–Leu* gene, and the 5′ end of the *NADH dehydrogenase 1* gene *(16S-Leu-nad1)*; nuclear markers: the 5′ end of the *18S rRNA* gene (*18S*); and an internal fragment of the *28S rRNA* gene (*28S*) Partial gene sequences were amplified by PCR using primers listed in Table S1 (Ober, 2002*; Ribera et al., 2010*; Shull et al., 2001*; Simon et al., 1994*), and following PCR amplification protocols listed in Table S2. PCRs were made in a 35 μl volume using EH2O: 18.8 μl, Buffer: 7.1 μl, dNTPS (2 mM): 3.5 μl, $MgCl_2$ (25 mM): 3.2 μl, Primer (20 mM): 1 μl forward and 1 μl reverse, polymerase 0.2 μl, and BSA 0.2 μl. For some samples with multiplied DNA bands, we ran PCR with 75 μl volume. Gel electrophoresis was done using special agarose (low EEO, for electrophoresis, Acros Organics), and then, separated bands were cut from gel and DNA was purified using the Thermo Scientific DNA purification kit. PCR products were sent to Macrogen Europe (Amsterdam, the Netherlands) for sequencing. Each fragment was sequenced in both directions using PCR amplification primers. The lengths of the PCR products (Amplicon length) generated with primers are listed in Table S1.

2.5 | Phylogeny inference and molecular dating

Geneious v. 5.6.7 (Kearse et al., 2012) and ChromasPro 2.1.3 (Technelysium, Tewantin, Australia) were applied to assemble sequences, as well as for editing and proofreading. Alignments were done using MEGA (Kumar et al., 2018). We concatenated all marker matrices in Mesquite version 3.6 (Maddison & Maddison, 2018). The aligned concatenated matrix contained 3540 characters (ch) including 739 ch for *16S*, 622 ch for *18S*, 984 ch for *28S*, and 1195 ch for *COI*. Mined sequences varied in length and starting positions within a gene; therefore, some characters are represented by gaps, for example, the longest sequence of the *COI* alignment was 857 ch. MEGA (Kumar et al., 2018) was used to find the best nucleotide substitution model and the optimal partitioning scheme for each marker. To reconstruct the phylogeny of *Duvalius* and related genera, we conducted Bayesian inference using MrBayes v. 3.2.7a (Huelsenbeck, & Ronquist, 2001). The optimal settings for our data involved four partitions, each using an independent nucleotide substitution model (*16S*: HKY+I+G; *18S*: JC+G; *28S*: K2+G; *COI*: GTR+I+G) (Alignment S1–S5). We ran two independent Bayesian runs, each with four MCMC chains, for 15 million generations with a sampling frequency of 3000. A relative burn-in was set to 25% and checked for the MCMC chain convergence in Tracer 1.7 (Rambaut et al., 2018). To check whether any marker creates unexpected noise in analyses, and to compare node supports, we performed Bayesian analyses for each individual marker and for combinations of two and three markers, in addition to concatenated matrices.

We ran maximum likelihood analyses (hereafter ML) with a separate substitution model for each of the four partitions (*16S*: HKY+I+G; *18S*: JC+G; *28S*: K2+G; *COI*: GTR+I+G) and ultrafast bootstrapping in IQ-tree 1.6.7 (Nguyen et al., 2014). We obtained node support values with 1000 bootstrap replicates (Hoang et al., 2018).

We employed BEAST2 (Bouckaert et al., 2019) to reconstruct time-calibrated phylogenies (chronograms). In BEAUti (Bouckaert et al., 2019), the bModelTest (Bouckaert & Drummond, 2017) was selected as the substitution model for each of the four gene partitions. bModelTest, a package implemented in BEAUti, uses a reversible jump MCMC that integrates over all substitution models available in the software (Bouckaert & Drummond, 2017). To time calibrate our phylogeny, we used molecular clock rates and models optimized for the beetle family Carabidae and regularly used for Trechini (Andújar et al., 2012). The *COI* partition used a strict clock with normal prior distribution (mean 0.0134, sigma 0.0015), the 16S partition used a strict clock with normal prior distribution (mean 0.0016, sigma 3e-4), while the *18S* and *28S* partitions ran under the same relaxed log-normal clock model with normal prior distribution (mean 0.0029, sigma 5e-4). The birth-death tree prior was used. BEAST analyses ran for 20 million MCMC generations with a sampling frequency of 2000.

Time-calibrated analyses can be sensitive to the inclusion or exclusion of outgroup taxa (Andújar et al., 2012). Therefore, to avoid any time-calibration biases introduced by the outgroup, we reconstructed another chronogram with settings as above, but this time using ingroup taxa only.

After examining the log files with Tracer 1.7 (Rambaut et al., 2018), we discarded 20% of the trees as burn-in and summarized the remainder of trees with TreeAnnotator (Bouckaert et al., 2019). The target tree was set as the Maximum clade credibility tree, and the node heights were set as median heights. All phylogenetic and molecular dating of BEAST and Bayesian analyses were performed on CIPRES (Miller et al., 2010), while maximum likelihood was run on IQ-TREE webserver (Trifinopoulos et al., 2016).

3 | RESULTS

3.1 | Taxonomy

***Duvalius* (*Duvalius*) *nezelensis* Muilwijk & Malek Hosseini** sp. nov.

(Figure 3a-e).

http://zoobank.org/urn:lsid:zoobank.org:act:53D2B6C8-8496-4B36-B2D3-A518FC4EE287

Type material

Holotype male labeled: "Iran Kohgiluyeh Va Boyer Ahmad, Zagros / Nezel cave, 12.vi.2018 / M. Porebrahim, S. Azizi, Z. Rozbehi, S. Rahideh, & J. Muilwijk leg." // "Holotype / *Duvalius* (*Duvalius*) *nezelensis* sp. nov. / Muilwijk & Malek Hosseini des. 2021" (black print on red label). Paratypes, one male labeled: "Iran, Kohgiluyeh va Boyer Ahmad, Zagros / Nezel cave, 15.xi.2016 / Mohammad Javad Malek Hosseini leg.";—one female labeled: "Iran, Kohgiluyeh va Boyer Ahmad, Zagros / Nezel cave 9.x.2017 / Tahami leg.";—three males and two females labeled: "Iran Kohgiluyeh Va Boyer Ahmad, Zagros / Nezel cave, 12.vi.2018 / M. Porebrahim, S. Azizi, Z. Rozbehi, S. Rahideh, & J. Muilwijk leg." // "Paratype / *Duvalius* (*Duvalius*) *nezelensis* sp. nov. / Muilwijk & Malek Hosseini des. 2021" (black print on red label). Holotype and female paratype deposited at HMIM, one female paratype at ZM–CBSU, one male paratype at NBCL, three males and one female paratypes at CMU.

Additional examined material

Duvalius (*D.*) *hetschkoi matilei* Deuve, 2000

Iran: Kerman Jiroft, Narab, 900 m, 16.xi.1999, Badii, Bar. Mof leg.; HMIM. 1 male.

Duvalius (*D.*) *kileri* Muilwijk & Malek Hosseini, 2016.

Iran: Kohgiluyeh Va Boyer Ahmad, Kiler cave, 150 km North West of Yasuj, 27.x.2011, N 31°17′96″, E 50°35′13″, 1610 m, Mohammad Javad Malek Hosseini leg., ZM–CBSU. Male holotype; — Kiler cave, 14.vi.2018, S. Rahideh & J. Muilwijk leg., HMIM, CMU. Three males and three females.

Duvalius (*D.*) *koeni* Muilwijk & Felix, 2008

Iran: Khuzestan, Pole-e Tang, 60 km NW Andimeshk, Loc. No. 284, 10–11.iv.1977, Exped. Nat. Mus. Praha. MNP. *male* holotype; —Lake Izeh, 01.iv.2007, Muilwijk leg., CMU. Female paratype.

Duvalius (*D.*) *mohammadzadehi* Muilwijk & Felix, 2008

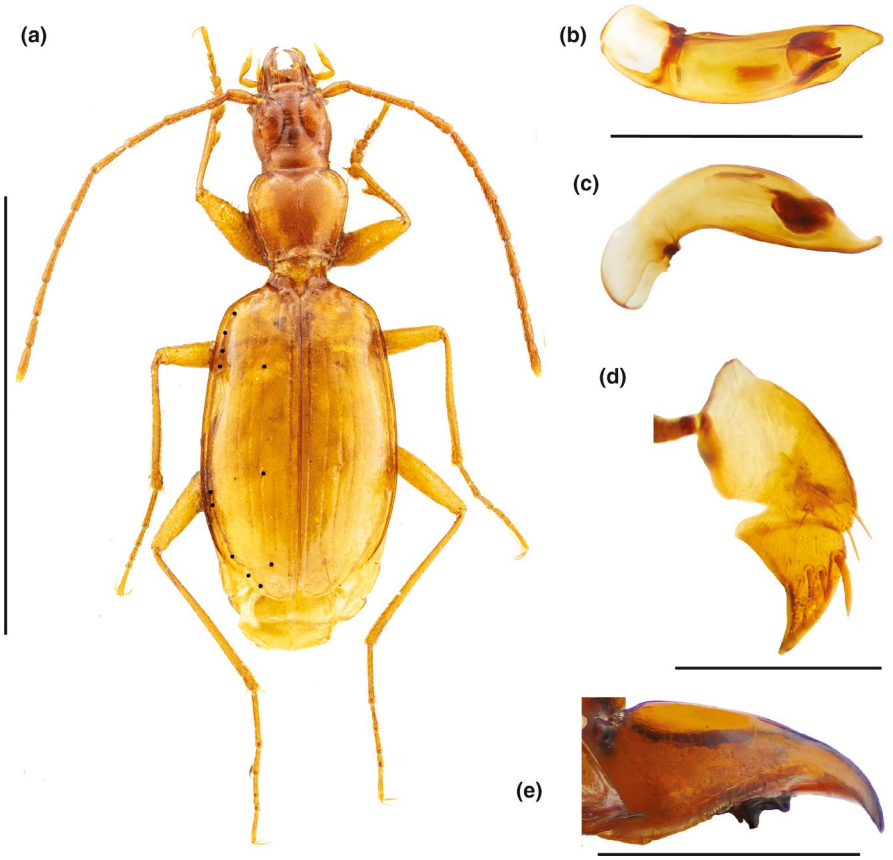

FIGURE 3 *Duvalius nezelensis*: (a) HT, habitus, scale: 4 mm, chaetotaxy indicated with black spots on elytra. (b) HT, median lobe median lobe, dorsal. (c) PT, median lobe median lobe, left lateral. scale: 1 mm. (d) PT, Gonocoxite and laterotergite IX, ventral, scale: 0.2 mm. (e) PT, right mandible ventral, scale: 0.5 mm

Iran: Fars, Estahban, 25.iv.2006, 2380 m, Muilwijk leg., MNP. Male holotype, one female paratype, CMU.

Description

(Figure 3), a large-sized anophthalmic, wingless *Duvalius* with upperside of head testaceous, pronotum, and elytra yellow. Appendages long. Fine hairs on genae, pronotum, lateral sides of elytra, and lateral sides of ventrites. Total length 5.48–6.15 mm, males: 5.53–5.89 mm (holotype 5.84 mm, average 5.73 mm, $n = 5$), females: 5.48–6.15 mm (average 5.71 mm, $n = 3$).

Head elongated, as long as wide, with slightly swollen genae narrowed to the neck; frontal furrows half-circular, impressed; eyes absent; very small ocular scars without pigment and covered by integument (in some individuals barely recognizable); genae with fine hairs; two pairs of long supraorbital setae, anterior pair just behind the middle and posterior pair in the basal part of frontal furrows; clypeus with two pairs of setae, labrum with three pairs of setae; right mandible with three teeth at the base, the first two teeth are along the ventral side, the third small flat tooth is located dorsally of the large one (as shown in Figure 3e), left mandible with a ridge of three very small teeth; apical border of ligula with eight setae, concave; antennae long and slender, reaching over the middle of elytra, covered with dense decumbent hair; antennomeres 3–7 nearly equally long.

Pronotum rounded anteriorly, then almost straight, slightly concave to hind angles (ratio PL/PW: 0.87–0.93 (HT: 0.91), wider than head; lateral sides rounded, slightly sinuate toward the acute upwards pointed hind angles, front angles rounded, obtuse; base with a slight indentation; lateral margin with two pairs of setae, anterolateral setae situated in the anterior fifth of the lateral margin, basolateral pair before hind angles; basal fovea short and moderate deep; lateral sides with fine hairs.

Elytra elongate (ratio EL/EW: 1.47–1.65; HT: 1.56), widest at the apical third, much wider than pronotum; basal line of the elytra clearly oblique; lateral furrows wide; all striae superficially and provided with superficial punctures; first stria of elytra curved back to the fifth stria. Scutellar stria not deepened. Sides with fine hairs, denser to the lateral sides. Elytra with a scutellar setiferous pore, three setiferous discal punctures (two discal in stria 3, one pre-apical in interstria 3), umbilicate series consist of eight setiferous pores, divided over three groups shown as black spots in Figure 3a. The humeral group consists of four pores at equal distance from each other. The second group of two pores is situated just behind the middle. The apical group consists also of two pores; angulo-apical punctures present.

Legs long, slender; femora and tibia with many tiny bristles, tarsi with dense decumbent hairs; protibiae with a longitudinal furrow dilated with fine apical hairs; protarsi in the male with two basal tarsomeres dilated, first tarsomere slightly denticulate inwards, second

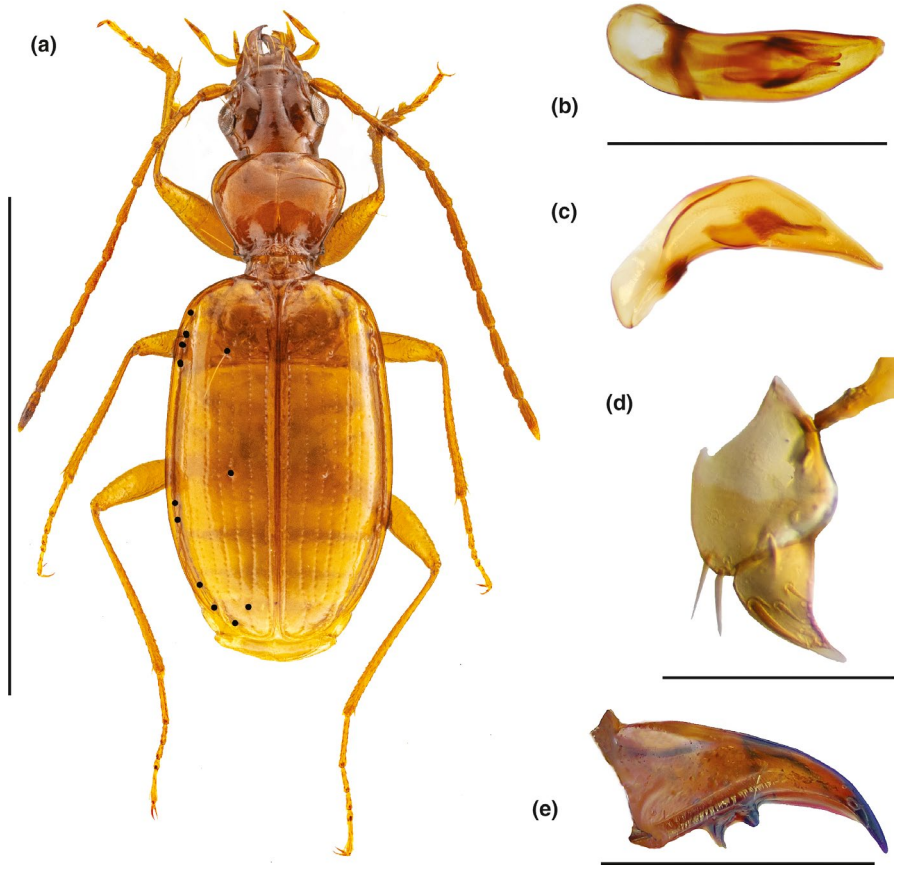

FIGURE 4 *Duvalius achaemenius*: (a) HT, habitus, scale: 4 mm, chaetotaxy indicated with black spots. (b) HT, median lobe, dorsal, scale: 1 mm (c) PT, median lobe, left lateral, scale: 1 mm. (d) PT, Gonocoxite and laterotergite IX, ventral, scale: 0.2 mm. (e) PT, right mandible ventral, scale: 0.5 mm

tarsomere with three very short, blunt dents along apical margin. Tarsal claws of front leg of normal size.

Ventral side: mentum with two short, blunt teeth; proepisternum and ventrites with fine hairs; ventrites 4–6 with a pair of paramedial setae. Along the apical border of the anal ventrite in both sexes also two setae.

Microsculpture: polygonal meshes on the head and pronotal disk, transversal meshes on lateral sides of pronotum, and dense transversal meshes on elytra.

Male genitalia as in Figure 3b,c: median lobe 1.25 mm long, in lateral view regularly curved and upwards sinuated at the apex; in dorsal aspect slightly sinuate in basic fifth, middle part parallel-sided, apex asymmetrical, triangular, tip rounded. Copulatory piece isotopic, consisting of two long sclerotized lateral parts, a horseshoe-shaped sclerotized median part and a sclerotized rectangular basal part embedded in a hyaline structure; in dorsal view, the symmetrical lateral lamellae enclose at the base the rectangular basal lamella and consist apical of dense sclerous scales; the horseshoe-shaped part ends apical in a tip, the hyaline structure is provided with scattered scales; in lateral view the lateral lamellae form apically a semicircle of dense sclerous scales, the horseshoe-shaped lamella is enclosed by the lateral lamellae and ends apically near the orifice in a hooked tip, the basal part forms a dorsal plate in the middle of the median lobe. Length of parameres about half of the length of median lobe, each paramere with four apical setae.

Female gonocoxites and laterotergites as in Figure 3d: few hairs on the gonocoxite, laterally with a big spine.

Differential diagnosis

D. nezelensis sp. nov. differs from all known Iranian *Duvalius* species by the absence of eyes, small elongated head, clearly longer appendages, more and longer pubescence on legs and antennae, the short hairs on the elytra and sides of the head, and the copulatory piece with an accessory horseshoe-shaped lamella (Figures 3–5).

Distribution and habitat

Known only from the type locality; the new species was collected on wet clay in the first hall of the Nezel cave, Zagros Mts., Southwestern Iran.

Etymology

Topotypic, the species epithet refers to the cave where the species was collected.

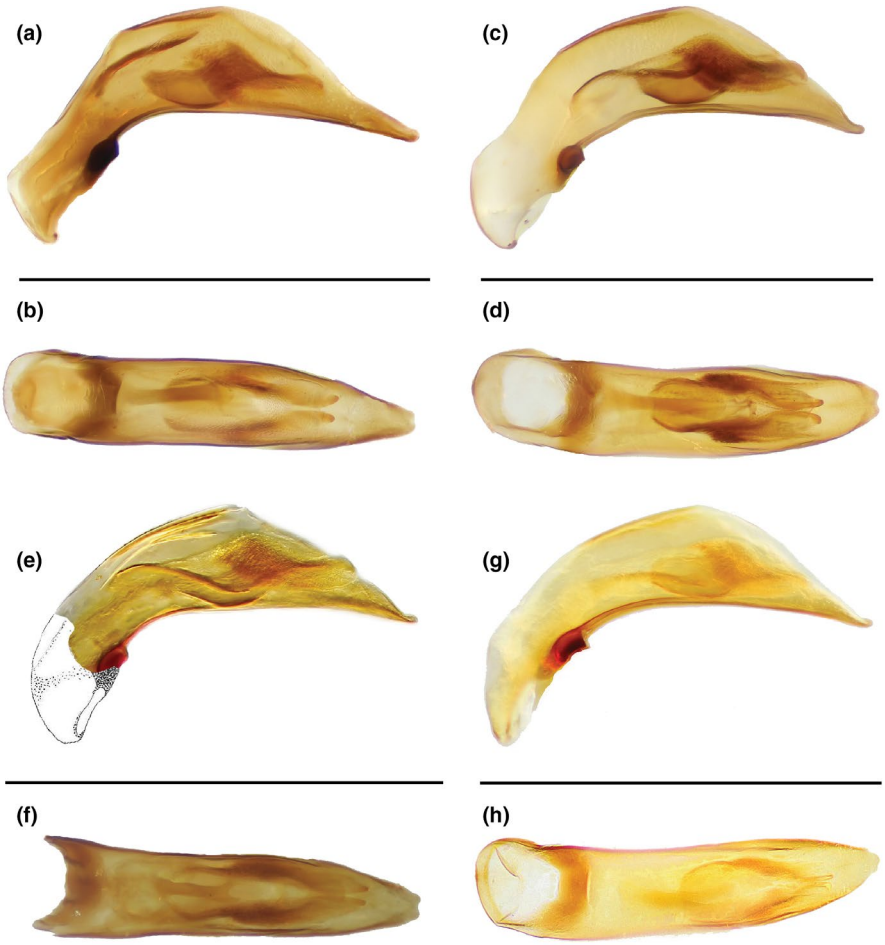

FIGURE 5 Median lobe of Iranian *Duvalius*. (a) *D. hetschkoi matilei*, median lobe, left lateral. (b) *D. hetschkoi matilei*, median lobe, dorsal. (c) *Duvalius* (*D.*) *kileri* median lobe, left lateral. (d) *Duvalius* (*D.*) *kileri* median lobe, dorsal, dorsal. (e) *Duvalius* (*D.*) *koeni*, median lobe, left lateral. (f) *Duvalius* (*D.*) *koeni*, median lobe PT, dorsal. (g) *Duvalius (D.) mohammadzadehi* HT median lobe, left lateral. (h) *Duvalius (D.) mohammadzadehi* HT median lobe, dorsal. Scale: 1 mm

***Duvalius* (*Duvalius*) *achaemenius* Muilwijk & Malek Hosseini** sp. nov. (Figure 4a-e).

http://zoobank.org/urn:lsid:zoobank.org:act:1F57B27C-43F8-40EA-B4D9-082E7F334BDF

Type material

Holotype male labeled: "Iran, Kohgiluyeh Va Boyer Ahmad / Suq cave near Suq / 16.vi.2018 / S. Rahideh & J. Muilwijk leg." // "Holotype / *Duvalius* (*Duvalius*) *achaemenius* sp. nov. Muilwijk & Malek Hosseini des. 2021" (black print on red label). Paratypes, male labeled: "Iran, Kohgiluyeh Va Boyer Ahmad / Suq cave near Suq / 31.iv.2017 / Yaser Fatemi leg.". —two males and one female labeled: "Iran, Kohgiluyeh Va Boyer Ahmad / Suq cave near Suq / 16.vi.2018, S. Rahideh & J. Muilwijk leg." // "Paratype / *Duvalius* (*Duvalius*) *achaemenius* sp. nov. Muilwijk & Malek Hosseini des. 2021" (black print on red label). Holotype deposited at HMIM, one male paratype at NBCL, two males and one female paratypes at CMU.

Additional examined material

The same material was used for this species as in the description of the previous species.

Description

Figure 4a: A medium-sized *Duvalius* with testaceous upper side and yellow appendices yellow. Pronotum shiny, head and elytra dull. Vestigial wings present. Total length 4.99–5.45 mm, males: 4.99–5.45 mm (holotype 5.43 mm, average 5.24 mm, $n = 3$), female: 5.13 mm).

Head wider than long; frontal furrows half-circular, impressed; eyes well developed, much larger than genae (1.32×); two pairs of long supraorbital setae, anterior pair above the eye and posterior pair in the basal part of frontal furrows; clypeus with two pairs of setae, labrum with three pairs of setae; right mandible with two large teeth at the base (as shown in Figure 4e), left mandible with a ridge of three very small teeth; apical border of ligula with eight setae, slightly convex; antennae long and slender, exceeding somewhat over middle of elytra, antennomeres 3–7 nearly equally long; antennomere 1 with a few setae, second half of antennomere with scattered setae, from antennomere three onwards more dense setae.

Pronotum cordiform (ratio PL/PW: 0.77–0.81 (HT: 0.77); wider than head; lateral sides rounded, slightly sinuate toward the acute upwards pointed hind angles, front angles rounded, obtuse; lateral margin with two pairs of setae, anterolateral setae situated in the

anterior third of the lateral margin, basolateral pair before hind angles; basal fovea short and deep, median line well marked.

Elytra subparallel (ratio EL/EW: 1.55–1.64; HT: 1.64), widest at apical third, humeri rounded; lateral furrows wide; striae 1–5 impressed, striae 6–7 superficially and striae 1–7 clearly punctured, first stria of elytra curved back to fifth stria, second stria reaching the apical puncture, stria 3–7 reaching to pre-apical setiferous discal puncture.

Elytra with a scutellar setiferous pore, three setiferous discal punctures (two discal in stria 3, one pre-apical in interstria 3), umbilicate series consist of eight setiferous pores, divided over three groups as shown as black spots in Figure 4a). The humeral group consists of four pores at equal distance from each other. The second group of two pores is situated just behind the middle. The apical group consists also of two pores; angulo-apical punctures present.

Microsculpture: head with reticulate and elytra with fine transverse meshes.

Legs: femora and tibia with some tiny bristles, tarsi with some decumbent hairs, protibiae with a longitudinal furrow on their dorsal side, slightly dilated with a fine apical hair; protarsi in the male with two basal tarsomeres dilated.

Ventral side: mentum tooth bifid; ventrites 4–6 with a pair of paramedial setae. Along the apical border of the anal ventrite in both sexes also two setae.

Male genitalia as in Figure 4b,c. Median lobe 0.98 mm long, median lobe in lateral view dorsal side strongly convex, with maximum width around the middle, tip rounded, in dorsal view basal part curved, apex asymmetrical, tip rounded. The copulatory piece consists of two sclerotized lateral parts and a sclerotized elongated basal part embedded in a hyaline structure; in dorsal view the symmetrical undulating lateral lamellae enclose partly the elongated basal lamella, and consist in the middle of dense sclerous scales and end apically in a tip, the elongated basal lamella is narrow in the middle and widened to the base and apex, the apex is more or less triangular; the hyaline structure is provided with scattered scales; in lateral view, the lateral lamellae are in the middle provided with dense sclerous scales, apically ending in a bended tip near the orifice, the undulating elongated basal lamella medio-dorsally situated.

Female gonocoxites and laterotergites as in Figure 4d. Gonocoxites with two visible hairs and a spine laterally.

Differential diagnosis

D. achaemenius sp. nov. (Figure 4) differs from *D. nezelensis* (Figure 3) by the presence of eyes; from all other Iranian *Duvalius* species by the form of the median lobe and copulatory piece (Figure 5a-h), from *Duvalius* (*D.*) *koeni* by more rounded humeri and less impressed striae and from *Duvalius* (*D.*) *koeni* and *Duvalius* (*D.*) *hetschkoi matilei* by reduced wings; from *Duvalius* (*D.*) *kileri* and *Duvalius* (*D.*) *mohammadzadehi* by more developed eyes.

Distribution and habitat

Known only from the type locality, the new species was found under wet stones about 50 m. from the entrance of the Suq cave, Zagros Mts., Southwestern Iran.

Etymology

The species epithet refers to the Achaemenid dynasty, a royal house of the Old Persian Empire.

3.2 | Key to the Iranian species of *Duvalius*

1- Eyes absent, pronotum slightly cordiform, habitus as in Figure 3a; copulatory piece with a horseshoe-shaped sclerotized median part Figure 3b, c;
.....*D. nezelensis* sp.nov.
- Eyes present, pronotum strongly cordiform; copulatory piece without a horseshoe-shaped sclerotized median part.
..... 2
2- Species with developed wings..... 3
- Species without reduced or without wings.
.....4
3- Eyes more prominent, clearly protruding; pronotum with acute upwards pointed hind angles; sides of elytra more or less parallel; median lobe as in Figure 5a, b.
.....*D. hetschkoi matilei* Deuve, 2000
- Eyes less prominent; hind angles pronotum less acute; sides of elytra more oval; median lobe as in Figure 5e, f.
.....*D. koeni* Muilwijk & Felix, 2008
4- Eyes not reduced; humeri regularly bent; striae moderately impressed; habitus as in Figure 4; apex of median lobe curved as in Figure 4b.
.....*D. achaemenius* sp.nov.
- Eyes reduced.
..... 5
5- Striae on elytra superficial; species from Fars; median lobe as in Figure 5f, g.
.....*D. mohammadzadehi* Muilwijk & Felix, 2008
- Striae on elytra impressed; species from Kohgiluyeh va Boyer Ahmad; median lobe as in Figure 5c, d.
.....*D. kileri* Muilwijk & Malek Hosseini, 2016.

3.3 | Annotated catalogue of *Duvalius* from Iran with a distribution map of the species (Figure 1)

Duvalius (*D.*) *achaemenius* **sp. nov.**; Kohgiluyeh Va Boyer Ahmad, Suq cave, 30°49′25.9" N, 50°25′37.9" E, altitude 812 m a.s.l.

Duvalius (*D.*) *hetschkoi matilei* Deuve, 2000; Bushehr, Ahram Omar, near the Persian Gulf, altitude 100 m a.s.l.; Kerman Jiroft, Narab, altitude 900 m a.s.l. 16.xi.1999 Badii, Bar. Mof.

Duvalius (*D.*) *kileri* Muilwijk & Malek Hosseini, 2016; Kohgiluyeh Va Boyer Ahmad, Kiler cave 150 km North West of Yasuj, 31°17′96" N, 50°35′13" E, altitude 1610 m a.s.l.

Duvalius (*D.*) *koeni* Muilwijk & Felix, 2008; Khuzestan, Pole-e Tang, 60 km NW Andimeshk; Khuzestan, Izeh.

Duvalius (*D.*) *mohammadzadehi* Muilwijk & Felix, 2008; Fars, Estahban, altitude 2380 m. a.s.l.

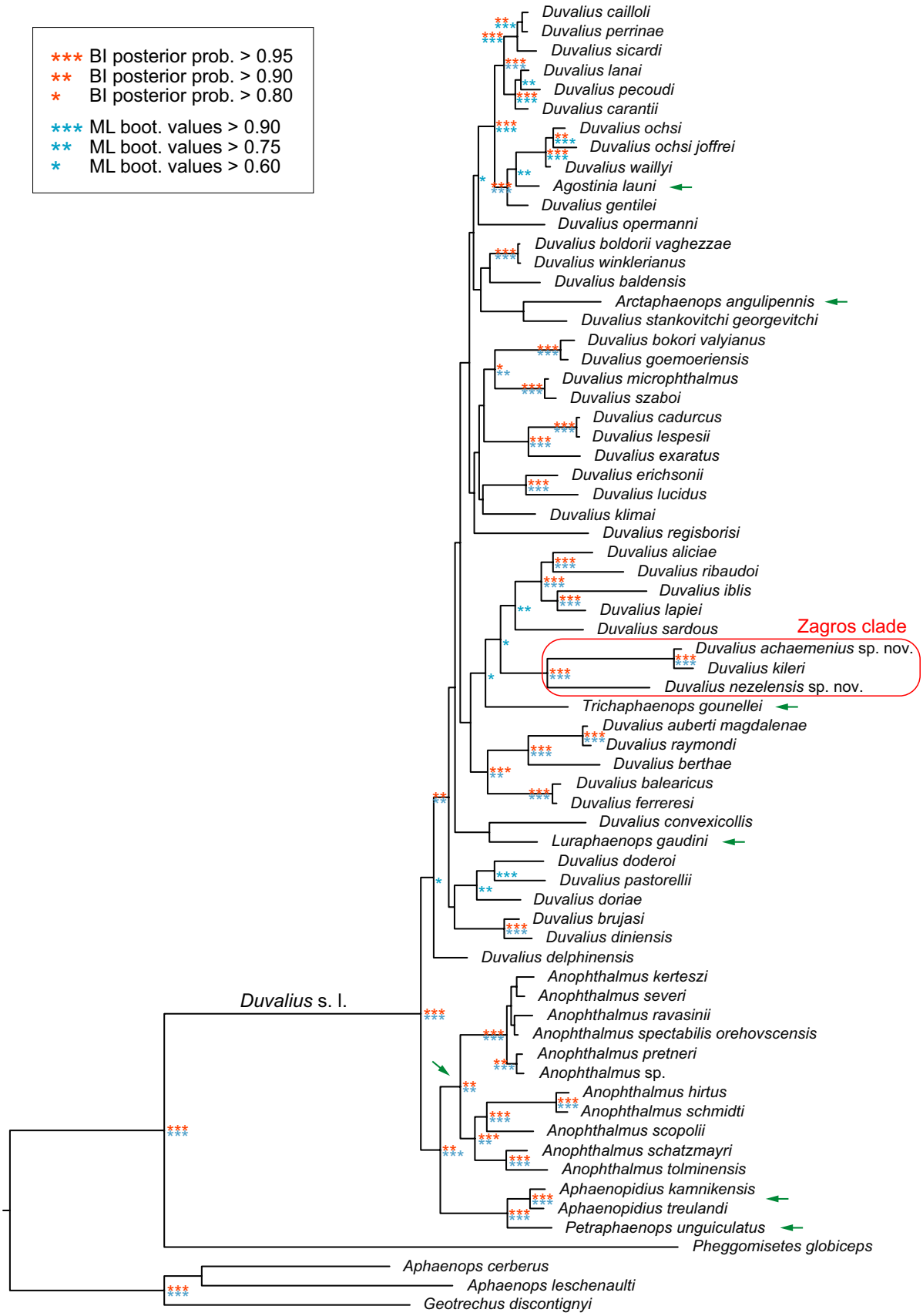

FIGURE 6 Phylogeny of the *Duvalius* lineage group of the Trechini beetles. The topology is from the Bayesian inference analysis, with all compatible groups. Colored asterisks mark both Bayesian inference (BI; orange) and maximum-likelihood (ML; blue) node supports. The red ellipse marks the highly supported Zagros clade. The relationships within Trechini are poorly resolved. Green arrows mark genera other than *Duvalius*

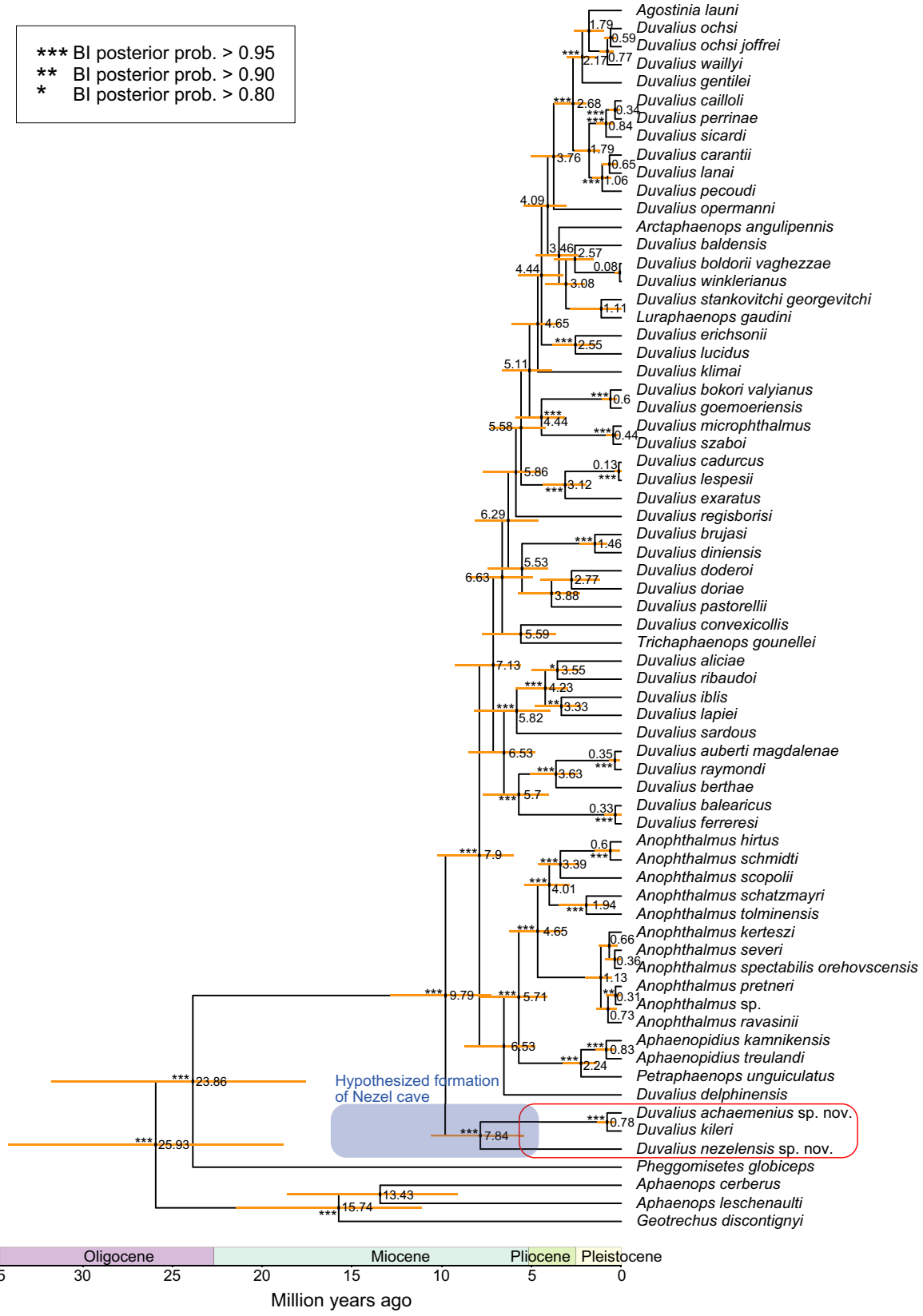

FIGURE 7 BEAST chronogram of the *Duvalius* lineage of the Trechini beetles, based on molecular clock rates for four markers. Orange bars on the nodes indicate 95% highest posterior probability density for node age. Asterisks indicate nodal support from BEAST. This chronogram suggests that Zagros clade split from the rest of *Duvalius* between 7.3 and 12.9 Ma (mean 9.7 Ma) in Late Miocene and soon thereafter diversified. *D. nezelensis* sp. nov. probably colonized the Nezel cave and developed its troglomorphic features between 5.4 and 10.6 Ma (mean 7.8 Ma) in Late Miocene and present time. The figure shows estimated time of the Nezel cave formation after Popov et al. (2004)

Duvalius (*Duvalius*) *nezelensis* **sp. nov.**; Kohgiluyeh va BoyerAhmad, Nezel cave, 30°47′28.62" N, 50°56′53.83" E, altitude 2307 m a.s.l.

3.4 | Phylogeny

All analyses strongly support the monophyly of the *Duvalius* species group from the Zagros Mts. labeled and discussed as the "Zagros clade", consisting of *D. kileri*, *D. achaemenius*, and *D. nezelensis*. They recover a sister relation of *D. nezelenzis* with *D. achaemenius* + *D. kileri* with high node support (Figures 6, 7 and S1–S3). However, the relationships within the *Duvalius* lineage of Trechini are poorly resolved in all Bayesian and ML analyses, and thus, the position of the Zagros clade cannot yet be resolved. This may be due to the lack of molecular data for most of the potentially sister candidates from the neighboring countries of Iran. Although poorly supported, both Bayesian and ML analyses consistently recover the Zagros clade as sister to a clade containing Algerian (*D. iblis* (Peyerimhoff, 1910), *D. lapiei* (Peyerimhoff, 1908)), Sicilian (*D. aliciae* Magrin, Baviera & Petrioli, 2007, *D. ribaudoi* Magrini, Petrioli & Degiovanni, 2010), and Sardinian (*D. sardous* (Dodero, 1917)) representatives (Figures 6, S1 and S2). This larger clade is sister to a troglobiotic species from France, *Trichaphaenops gounellei* (Bedel, 1879). However, the support for this relationship is relatively weak. One further inclusive node in this phylogeny is also weakly supported, but contains a clade sister to the above with a well-structured, and supported clade of Mediterranean, troglobiotic *Duvalius* species, including the type of the genus, *D. raymondi* Delarouzée, 1859.

The BEAST chronogram shows a phylogenetic proximity of the Zagros clade quite different from the above phylogenies. This analysis recovers the Zagros *Duvalius* clade as sister to the entire *Duvalius* lineage. However, we only use this BEAST analysis to test the timing of the major splits rather than as an alternative topological hypothesis of the relationship of the Zagros clade with other *Duvalius*. BEAST estimates the split of the Zagros clade to have occurred between 7.3 and 12.9 Ma (mean 9.7 Ma) in Late Miocene, which is congruent with the estimated time by Faille et al. (2013). The diversification of the Zagros clade is estimated to have occurred between 5.4 and 10.6 Ma (mean 7.8 Ma) in Late Miocene for the split of *D. nezelensis* from its sister group, and more recently in Middle Pleistocene between 0.4 and 1.3 Ma (mean 0.78 Ma) for the split of *D. achaemenius* and *D. kileri* (Figure 7). According to our BEAST estimation, the colonization of the subterranean environment by *D. nezelensis* must have occurred at any recent time since the Late Miocene (7.8 Ma) (Figure 7). Multiple, independent cases of eye loss are already well known in the *Duvalius* clade (Faille et al., 2013, 2018). The alternative explanation, that the ancestor of Zagros clade was already a cave-dweller, is unlikely because the implied ancestor to all *Duvalius* species would have to be spread in caves over a vast area of the Old World, which are clearly not interconnected. Our chronogram inferred the separation of the *Duvalius* group from the basal Trechini to have occurred between 18 and 32 Ma (mean 24 Ma) in late Oligocene (Figure 7), congruent with Faille et al. (2013) who estimated this split at 30 Ma. The alternative BEAST analysis with ingroups only produced comparable time estimates (Figure S3).

4 | DISCUSSION

In this study, we investigate cave-dwelling beetles of Zagros Mts in south-western Iran with the goals to make a three-pronged advancement in our understanding of the regional biodiversity: i) to aid in new species discovery of troglobiotic beetles; ii) to obtain a dated phylogeny of selected beetle taxa that would enable estimating the timing of cave colonization by beetles; and iii) to comment on the current knowledge of troglobiotic Iranian fauna more broadly.

4.1 | Discovery of troglobiotic beetles

Although Coleoptera and especially carabids have many representatives in subterranean environments, no troglobiotic carabid beetle has been discovered from Iran prior to this study and the only known troglobiotic coleopteran from Iran was the tenebrionid *Foranotum perforatum* (Nabozhenko & Sadeghi, 2017). This seemingly low species richness of cave-dwelling beetles in Iran is likely an artifact stemming from lack of focused research on this fauna. Most caves of the country that might potentially harbor troglobiotic beetles are not easy to reach, and there are no particular surveys on Iranian cave beetles. Moreover, given the vastness of the country and extension of karstic areas from north to south, an extensive study would require tremendous effort. After our discovery of two new species, a total of six *Duvalius* species are known in Iran. Of these, only *D. nezelensis* sp. nov. is a troglobiont. No doubt, we expect the presence of other new species in Iran, particularly from subterranean environments. However, our discovery of one new non-troglobiotic species, *D. achaemenius* sp. nov., and its closely related troglobiont, *D. nezelensis* sp. nov., is the first step toward a better understanding of the phylogeny and the origin of Iranian *Duvalius*.

Beside the absence of eyes and long appendages, the most striking features of *D. nezelensis* sp. nov. is the deviant shape of the copulatory piece in the median lobe. However, the chaetotaxy does not differ from other *Duvalius* species. The four previously known species (*D. hetschkoi matilei*, *D. kileri*, *D. koeni*, and *D. mohammadzadehi*) and the newly described *D. achaemenius* species are morphologically alike and can be described as the *hetschkoi* species group. The setiferous punctures of the series umbilicata and copulatory piece in the median lobe of the Iranian specimens match the description of the genus *Duvalius*, and differ from other genera of the *Duvalius* lineage (Casale & Laneyrie, 1982).

4.2 | Phylogeny and evolutionary history of the Zagros clade

Our study adds to phylogenetic resolution of Trechinae by adding three *Duvalius* species from Iran. However, incomplete sampling of *Duvalius* lineage species from all around the Palearctic from Western Europe to Caucasus and from Iran to China (no molecular data exist for over 80% of described species) does not allow us to resolve the

phylogeny of this vast lineage. The genus *Duvalius* contains over 300 described species and is among the most species-rich genera of the Trechini (Belousov, 2017). Faille et al. (2011; 2013; 2018) hypothesized that the *Duvalius* lineage, consisting of eight "genera," was monophyletic. Our phylogenies are consistent with a large *Duvalius* clade (Delić et al., 2020; Faille et al., 2013, 2018) and confirm non-monophyly of the genera nested within as found in previous analyses (Delić et al., 2020; Faille et al., 2013, 2018). In other words, *Duvalius* is paraphyletic with respect to these other genera. Therefore, a genus level taxonomy of *Duvalius* will require multiple redefinitions. Rather than fixing the *Duvalius* taxonomy, we here focus our discussion on the evolutionary implications of the Zagros clade relationships.

Our molecular analyses agree on the monophyly of the Zagros clade that unites both newly discovered species with the troglophilic *D. kileri*. We hypothesize that this clade will also include the three species of *Duvalius* from Iran (*D. hetschkoi matilei*, *D. koeni*, and *D. mohammadzadehi*) that were not included in our phylogeny. This expectation seems warranted by morphological resemblance, and geographic proximity of the included and omitted Iranian *Duvalius*.

Due to the lack of species from the neighboring countries, our analyses cannot unequivocally pinpoint the immediate phylogenetic relative of the Zagros clade. Although ML and Bayesian topologies both suggest this clade to consist of five species from Algeria, Sicily, and Sardinia, the node supports are weak. In addition, BEAST analyses consistently place the Zagros clade as sister to a vast assemblage of *Duvalius*. While we place more confidence in the ML and Bayesian topologies for sister group relationships, and resort to BEAST more for estimated time of major splits, this inconsistency in topologies precludes a more resolute conclusion as to which of the West Palaeartic clades of *Duvalius* is the closest relative to the Zagros clade.

According to our chronogram, the three species from Zagros shared the most recent common ancestor between 7.3 and 12.9 Ma (mean 9.7 Ma) in the Late Miocene. This implies that *D. nezelensis* developed its troglomorphic features between the Late Miocene and today. In fact, considering that the estimated split overlaps with the potential time frame of the Nezel cave formation (Figure 7; Popov et al., 2004), the cave colonization by *D. nezelensis* is likely to have taken place around the time of this hypothesized split, and this must have been followed by accrual of troglomorphies as described in the contemporary *D. nezelensis* population. The basal diversification of Zagros clade is estimated to have occurred between 5.4 and 10.6 Ma (mean of 7.8 Ma) in the Late Miocene, and the recent split occurred between 0.4 and 1.3 Ma (mean 0.78 Ma) in the Late Pleistocene. Given the estimated 7 million years between these two splits, the inclusion of other Iranian *Duvalius* species as well as those from neighboring countries could illuminate future studies about the evolutionary events of this period.

A more recent cave colonization of species of the *hetschkoi* species group in Pleistocene is implied by *D. achaemenius* sp. nov. and *D. kileri*. This agrees with Hernando (1999) who hypothesized a recent colonization of the subterranean environment by *D. hetschkoi* in Afghanistan. The speciation of the *hetschkoi* species group in Iran is limited to a small area in the Zagros Mountains. *D. kileri* has several adaptations such as reduced wings, small eyes, long antennae (Malek Hosseini et al., 2016) that implies this species has had a life in darkness but not long enough to completely obtain troglomorphic features. On the other hand, *D. achaemenius* sp. nov. shows no troglomorphies, and this species may have had recent or no continuous history in hypogean environments. This conclusion agrees with the qualities of Suq cave, the collection locality of *D. achaemenius* sp. nov. being a shallow cavern without absolute darkness.

All evidence combined point to our conclusion that the Zagros clade represents an independent evolutionary origin of subterranean colonization and troglomorphic evolution. As pointed out by Faille et al. (2013), multiple colonizations of the subterranean environment by *Duvalius* have occurred elsewhere. We see the alternative explanation that all *Duvalius* may have shared a subterranean ancestor, unlikely. First, such scenario would imply an unusually broad area of occupancy of this hypothetical ancestor. Second, this vast area would be spread over karsts of different ages and origins that are clearly not interconnected. Third, such scenario would imply numerous cases of re-emergence from subterranean environments. For these reasons, we find the alternative explanation as highly unlikely. Rather, the *Duvalius* lineage contains beetles predisposed for living underground. The development of karstic systems then triggers numerous and repeated cases of cave colonization.

4.3 | Iranian troglobiotic fauna species richness

Karstic carbonate formations cover about 11% of Iran's land where over 2000 caves have been registered (Raeisi et al., 2012). Nonetheless, Iran's subterranean fauna remains poorly known with only about 45 reported troglobiotic species. Of these, most are crustaceans (38), while the other represent fishes, gastropods, arachnids, and myriapods (Bargrizaneh et al., 2021; Fatemi et al., 2019; Malek Hosseini & Zamani, 2017). Most of these species have been discovered from Zagros karst. Clearly, the currently reported diversity of Iranian troglofauna is a vast underestimation. Compared to some karstic areas such as the Dinaric or the Balkan Peninsula (Sket et al., 2004), the areas studied, the number of studies and discovered troglobionts in Iran are very low. Considering ours and similar ongoing biospeleological research efforts, the detection of additional undescribed troglobiotic diversity, perhaps even troglobiotic hotspots in Iran, are possible. Such research effort is important for the understanding of the regional troglofaunal including the colonization of subterranean environments in different parts of the Iranian karst for both terrestrial and aquatic fauna, as well as for inclusion of Iranian subterranean biology within a context of general processes that shape cave colonization and present-day patterns of subterranean biodiversity.

ACKNOWLEDGMENTS

We thank Mohadeseh Sadat Tahami for loaning a paratype of *D. nezelensis* sp. nov, Saber Sadeghi for loaning the holotype of *D. kileri*, Jiří

Hájek for loaning type material of *D. koeni* and *D. mohammadzadehi*, Mehdi Poorebrahim, Shahab Azizi, Yaser Fatemi and Saadat Rahideh for field assistance. We thank Ron Felix and Teo Delić for comments on our manuscript, and Arnaud Faille for his comprehensive and expert review. We are thankful to Jean-François Flot for the preparation of the second abstract in the French language. This study was supported by grants of the Uyttenboogaart-Eliasen Stichting (grant number 2017.12.03), the Biotechnical Faculty of the University of Ljubljana for assistance in doctoral research, and in part by the Slovenian Research Agency (grants P1-0236, P1-0255, J1-9163, and J1-1703).

ORCID

Mohammad Javad Malek-Hosseini https://orcid.org/0000-0001-7411-2150
Jan Muilwijk https://orcid.org/0000-0002-0230-226X
Matjaž Gregorič https://orcid.org/0000-0002-4882-4282
Matjaž Kuntner https://orcid.org/0000-0002-0057-2178
Klemen Čandek https://orcid.org/0000-0002-5729-2943

REFERENCES

These references with '*', are related to the supporting information.

Agard, P., Omrani, J., Jolivet, L., Whitechurch, H., Vrielynck, B., Spakman, W., Monié, P., Meyer, B., & Wortel, R. (2011). Zagros orogeny: A subduction-dominated process. *Geological Magazine*, *148*, 692–725. https://doi.org/10.1017/S001675681100046X

Andújar, C., Serrano, J., & Gómez-Zurita, J. (2012). Winding up the molecular clock in the genus *Carabus* (Coleoptera: Carabidae): Assessment of methodological decisions on rate and node age estimation. *BMC Evolutionary Biology*, *12*, 40. https://doi.org/10.1186/1471-2148-12-40

Bargrizaneh, Z., Fišer, C., & Esmaeili-Rineh, S. (2021). Groundwater amphipods of the genus *Niphargus* Schiødte, 1834 in Boyer-Ahmad region (Iran) with description of two new species. *Zoosystema*, *43*, 127–144. https://doi.org/10.5252/zoosystema2021v43a7

Belousov, I. A. (2017). Trechini. In I. Löbl, & D. Löbl (Eds.), *Catalogue of Palearctic Coleoptera*, *Vol. 1. Archostemata – Myxophaga – Adephaga* (pp. 357–455). Revised and Updated Edition. Brill, Leiden

Bouckaert, R. R., & Drummond, A. J. (2017). bModelTest: Bayesian phylogenetic site model averaging and model comparison. *BMC Evolutionary Biology*, *17*, 1–11. https://doi.org/10.1186/s12862-017-0890-6

Bouckaert, R., Vaughan, T. G., Barido-Sottani, J., Duchêne, S., Fourment, M., Gavryushkina, A., Heled, J., Jones, G., Kühnert, D., De Maio, N., Matschiner, M., Mendes, F. K., Müller, N. F., Ogilvie, H. A., du Plessis, L., Popinga, A., Rambaut, A., Rasmussen, D., Siveroni, I., … Drummond, A. J. (2019). BEAST 2.5: An advanced software platform for Bayesian evolutionary analysis. *PLOS Computational Biology*, *15*, 1–28. https://doi.org/10.1371/journal.pcbi.1006650

Bousquet, Y. (2012). Catalogue of Geadephaga (Coleoptera, Adephaga) of America, north of Mexico. *ZooKeys*, *245*, 1–1722. https://doi.org/10.3897/zookeys.245.3416

Casale, A. (1979). Un nuovo *Duvalius* dell'Armenia turca (Coleoptera, Carabidae, Trechinae). *Bollettino Dei Musei Di Zoologia Ed Anatomia Comparata Della R. Università Di Torino*, *7*, 145–152.

Casale, A., & Laneyrie, R. (1982). Trechodinae et Trechinae du monde. Tableau des sous familles, tribus, séries phylétiques, genres, et catalogue général des espèces. *Mémoires de Biospéologie*, *9*, 1–226.

Cucchi, F., & Zini, L. (2003). Gypsum Karst of Zagros Mountains (I. R. Iran). *Acta Carsologica*, *32*, 69–82. https://doi.org/10.3986/ac.v32i1.365

Delić, T., Kapla, A., & Colla, A. (2020). Orogeny, sympatry and emergence of a new genus of Alpine subterranean Trechini (Coleoptera: Carabidae). *Zoological Journal of the Linnean Society*, *189*, 1217–1231. https://doi.org/10.1093/zoolinnean/zlz157

Deuve, T. (2000). La vie déserticole dans le genre *Duvalius* Delarouzée, 1854. Description d'une forme macroptère du Golfe Persique (Coleoptera, Trechidae). *Revue Francaise D'entomologie (N.S.)*, *22*, 159–163.

Faille, A., Casale, A., Balke, M., & Ribera, I. (2013). A molecular phylogeny of Alpine subterranean Trechini. *BMC Evolutionary Biology*, *13*, 248.

Faille, A., Casale, A., Hernando, C., Mouloud, S. A., & Ribera, I. (2018). Tectonic vicariance versus Messinian dispersal in western Mediterranean ground beetles. *Zoologica Scripta*, *47*, 556–581. https://doi.org/10.1111/zsc.12301

Faille, A., Casale, A., & Ribera, I. (2011). Phylogenetic relationships of western Mediterranean subterranean *Trechini groundbeetles* (Coleoptera: Carabidae). *Zoologica Scripta*, *40*, 282–295. https://doi.org/10.1111/j.1463-6409.2010.00467.x

Fatemi, Y., Malek-Hosseini, M. J., Falniowski, A., Hofman, S., Kuntner, M., & Grego, J. (2019). Description of a new genus and species as the first gastropod species from caves in Iran. *Journal of Cave and Karst Studies*, *81*, 233–243. https://doi.org/10.4311/2019LSC0105

Hernando, C. (1999). *Duvalius lindbergi orbayi* ssp. nov. from the Karakorum in Pakistan (Coleoptera: Carabidae). 4 pp. *Entomological Problems*, *30*(1), 53–56.

Hoang, D. T., Vinh, L. V., Flouri, F., Stamatakis, A., Haeseler, A., & Minh, B. Q. (2018). MPBoot: Fast phylogenetic maximum parsimony tree inference and bootstrap approximation. *BMC Evolutionary Biology*, *18*, 1–11. https://doi.org/10.1186/s12862-018-1131-3

Huelsenbeck, J. P., & Ronquist, F. (2001). MRBAYES: Bayesian inference of phylogenetic trees. *Bioinformatics*, *17*, 754–755. https://doi.org/10.1093/bioinformatics/17.8.754

Jamalpour, M., Hamdi, B., & Armoon, A. (2017). Lithostratigraphy and biostratigraphy of the Sarvak formation in wells no. 2, 16 and 66 of Rag-e-Safid oilfield in the Southwest of Iran. *Open Journal of Geology*, *7*, 806–821. https://doi.org/10.4236/ojg.2017.76055

Jeannel, R. (1928). *Monographie des Trechinae. Morphologie comparée et distribution d'un groupe de Coléoptères. Troisième Livraison: Les Trechini cavernicoles* (Vol. *35*, 1–808). Société entomologique de France.

Kearse, M., Moir, R., Wilson, A., Stones-Havas, S., Cheung, M., Sturrock, S., Buxton, S., Cooper, A., Markowitz, S., Duran, C., Thierer, T., Ashton, B., Meintjes, P., & Drummond, A. (2012). Geneious Basic: An integrated and extendable desktop software platform for the organization and analysis of sequence data. *Bioinformatics*, *28*, 1647–1649. https://doi.org/10.1093/bioinformatics/bts199

Kryzhanovskij, O. L., Belousov, I. A., Kabak, I. I., Kataev, B. M., Makarov, K. V., & Shilenkov, V. G. (1995). *A Checklist of the ground-beetles of Russia and adjacent lands (Insecta, Coleoptera, Carabidae)*. Pensoft Publishers.

Kumar, S., Stecher, G., Li, M., Knyaz, C., & Tamura, K. (2018). MEGA X: Molecular evolutionary genetics analysis across computing platforms. *Molecular Biology and Evolution*, *35*, 1547–1549. https://doi.org/10.1093/molbev/msy096

Maddison, D. R., Kanda, K., Boyd, O. F., Faille, A., Porch, N., Erwin, T. L., & Roig-Juñent, S. (2019). Phylogeny of the beetle supertribe Trechitae (Coleoptera: Carabidae): Unexpected clades, isolated lineages, and morphological convergence. *Molecular Phylogenetics and Evolution*, *132*, 151–176. https://doi.org/10.1016/j.ympev.2018.11.006

Maddison, W., & Maddison, D. (2018). *Mesquite: A modular system for evolutionary analysis version 570*. http://www.mesquiteproject.org

Malek Hosseini, M. J., Muilwijk, J., Sadeghi, S., & Bakhshi, Y. (2016). The Carabid fauna of caves in the southern Zagros Mountains and description of *Laemostenus* (*Antisphodrus*) aequalis nov. sp. and *Duvalius kileri* nov. sp. from Kohgiluyeh Va Boyer Ahmad Province, Iran (Coleoptera: Carabidae). *Entomofauna*, *37*, 185–204.

Malek-Hosseini, M. J., & Zamani, A. (2017). A checklist of subterranean arthropods of Iran. *Subterranean Biology*, *2*, 19–46. https://doi.org/10.3897/subtbiol.21.10573

Miller, M. A., Pfeiffer, W., & Schwartz, T. (2010). Creating the CIPRES Science Gateway for inference of large phylogenetic trees. In *Proceedings of the Gateway Computing Environments Workshop (GCE), New Orleans, LA* (pp. 1–8). https://doi.org/10.1109/GCE.2010.5676129

Muilwijk, J., & Felix, R. (2008). Description of three new species of the tribe Trechini (Col: Carabidae) from south Iran. *Journal of Entomological Society of Iran*, *28*, 79–85.

Nabozhenko, M., & Sadeghi, S. (2017). *Foranotum perforatum* gen. et sp. nov.—a new troglobitic darkling beetle (Coleoptera: Tenebrionidae: Kuhitangiinae: Foranotini trib. nov.) from a cave in Southern Zagros, Iran. *Zootaxa*, *4338*, 163–172.

Nguyen, T., Schmidt, H. A., von Haeseler, A., & Minh, B. Q. (2014). IQ-TREE: A fast and effective stochastic algorithm for estimating maximum-likelihood phylogenies. *Molecular Biology and Evolution*, *32*, 268–274. https://doi.org/10.1093/molbev/msu300

*Ober, K. A. (2002). Phylogenetic relationships of the carabid subfamily Harpalinae (Coleoptera) based on molecular sequence data. *Molecular Phylogenetics and Evolution*, *24*, 228–248. https://doi.org/10.1016/s1055-7903(02)00251-8

Parnian, B., Ahmadi, V., Saroii, H., & Bahrami, M. (2019). Biostratigraphy and palaeodepositional model of the Sarvak Formation in the Fars Zone, Zagros, Iran. *Journal of Himalayan Earth Sciences*, *52*, 197–216.

Popov, S. V., Rögl, F., Rozanov, A. Y., Steiniger, F. F., Shcherba, I. G., & Kovac, M. (2004). Lithological-paleogeographic maps of Paratethys 10 maps late Eocene to Pliocene. *Courier Forschungsinstitut Senckenberg*, *250*, 1–46.

Raeisi, E., Ghazy, S., & Laumanns, M. (2012). *Iran cave directory* (Vol. 45–46, 3rd ed., 315 p.). Berliner Höhlenkundliche Berichte.

Rambaut, A., Drummond, A. J., Xie, D., Baele, G., & Suchard, M. A. (2018). Posterior summarization in Bayesian phylogenetics using Tracer 1.7. *Systematic Biology*, *67*, 901–904. https://doi.org/10.1093/sysbio/syy032

Razin, P., Taati, F., & van Buchem, F. S. P. (2010). Sequence stratigraphy of Cenomanian-Turonian carbonate platform margins (Sarvak Formation) in the High Zagros, SW Iran: An outcrop reference model for the Arabian Plate. *Geological Society Special Publication*, *329*, 187–218. https://doi.org/10.1144/SP329.9

*Ribera, I., Fresneda, J., Bucur, R., Izquierdo, A., Vogler, A. P., Salgado, J. M., & Cieslak, A. (2010). Ancient origin of a Western Mediterranean radiation of subterranean beetles. *BMC Evolutionary Biology*, *10*, 1–14. https://doi.org/10.1186/1471-2148-10-29

Setudehnia, A. (1973). Geological map of Dedasht, scale 1:100,000. *National Iranian Oil Company, Exploration Directorate*.

*Shull, V. L., Vogler, A. P., Baker, M. D., Maddison, D. R., & Hammond, P. M. (2001). Sequence alignment of 18S ribosomal RNA and the basal relationships of adephagan beetles: Evidence for monophyly of aquatic families and the placement of Trachypachidae. *Systematic Biology*, *50*, 945–969. https://doi.org/10.1080/10635150175346289 4

*Simon, C., Frati, F., Beckenbach, A., Crespi, B., Liu, H., & Flook, P. (1994). Evolution, weighting, and phylogenetic utility of mitochondrial gene-sequences and a compilation of conserved polymerase chain-reaction primers. *Annals of the Entomological Society of America*, *87*, 651–701. https://doi.org/10.1093/aesa/87.6.651

Sket, B., Paragamian, K., & Trontelj, P. A. (2004). Census of the obligate subterranean fauna in the Balkan Peninsula. In H. I. Griffiths, & B. Krystufek (Eds.), *Balkan biodiversity – Pattern and process in Europe's biodiversity hotspot* (pp. 309–322). Kluwer Academic Publishers.

Tahami, M. S., Muilwijk, J., Lohaj, R., & Sadeghi, S. (2017). Study of *Laemostenus* species across with the description of seven new cavernicolous species and notes on subgenus *Iranosphodrus* (Coleoptera: Carabidae: Sphodrini). *Zootaxa*, *4344*, 115–136. https://doi.org/10.11646/zootaxa.4344.1.4

Trifinopoulos, J., Nguyen, L. T., von Haeseler, A., & Minh, B. Q. (2016). W-IQ-TREE: A fast online phylogenetic tool for maximum likelihood analysis. *Nucleid Acids Research*, *44*(W1), W232–W235. https://doi.org/10.1093/nar/gkw256

Vandel, A. (1964). *Biospéologie. La Biologie des Animaux Cavernicoles*. Gauthier- Villars.

Vatandoust, S., Mousavi-Sabet, H., Geiger, M. F., & Freyhof, J. (2019). A new record of Iranian subterranean fishes reveals the potential presence of a large freshwater aquifer in the Zagros Mountains. *Journal of Applied Ichthyology*, *35*, 1269–1275. https://doi.org/10.1111/jai.13964.

Vidergar, N., Toplak, N., & Kuntner, M. (2014). Streamlining DNA barcoding protocols: Automated DNA extraction and a new cox1 primer in arachnid systematics. *PLoS One*, *9*, e113030. https://doi.org/10.1371/journal.pone.0113030

Zagmajster, M., Culver, D. C., & Sket, B. (2008). Species richness patterns of obligate subterranean beetles (Insecta: Coleoptera) in a global biodiversity hotspot – effect of scale and sampling intensity. *Diversity and Distributions*, *14*, 95–105. https://doi.org/10.1111/j.1472-4642.2007.00423.x

SUPPORTING INFORMATION

Additional supporting information may be found in the online version of the article at the publisher's website.

Table S1. Primer details with targeted gene, primer names (F: forward; R: reverse) and sequences, amplicon lengths, and reference information.

Table S2. PCR amplification protocols.

Table S3. Taxonomic and gene information (GenBank accession numbers) data and the proportion of missing data for the 68 taxa used in our analyses.

Figure S1. Phylogeny of the *Duvalius* sensu lato group of the Trechini beetles, obtained by Bayesian inference, with all compatible groups and posterior probability supports for all nodes.

Figure S2. Phylogeny of the *Duvalius* sensu lato group of the Trechini beetles, obtained by IQ-tree, with bootstrap supports for all nodes.

Figure S3. BEAST chronogram of the *Duvalius* lineage of the Trechini beetles for ingroup taxa only.

Alignment S1. Nexus matrix of concatenated *16S*, *18S*, *28S* and *COI* sequences.

Alignment S2. Fasta file of *16S* sequences used in our analyses.

Alignment S3. Fasta file of *18S* sequences used in our analyses.

Alignment S4. Fasta file of *28S* sequences used in our analyses.

Alignment S5. Fasta file of *COI* sequences used in our analyses.

How to cite this article: Malek-Hosseini, M. J., Muilwijk, J., Gregorič, M., Kuntner, M., & Čandek, K. (2021). First insights into the origin of Iranian cave beetle diversity with description of two new species of the genus *Duvalius* (Carabidae). *Journal of Zoological Systematics and Evolutionary Research*, 59, 1453–1469. https://doi.org/10.1111/jzs.12537

APPENDIX 1

Specimen list of examined individuals, with collection and locality info, museum collection information, and genbank accession numbers

Duvalius species	Collection details	COI	16S	18S	28S
D. achaemenius sp. nov.	1 male, holotype, Iran, Kohgiluyeh Va Boyer Ahmad, Suq, Suq cave, 30°49′25.9″ N, 50°25′37.9″ E, 812 m, 16.vi.2018, HMIM, Rahideh, S., & Muilwijk, J.	–	–	–	–
D. achaemenius sp. nov.	1 male, paratype, Iran, Kohgiluyeh Va Boyer Ahmad, Suq, Suq cave, 30°49′25.9″ N, 50°25′37.9″ E, 812 m, 31.iv.2017 / CMU, Fatemi, Y.	MZ033000	MZ042533	MZ042980	MZ043751
D. achaemenius sp. nov.	1 male, paratype, Iran, Kohgiluyeh Va Boyer Ahmad, Suq, Suq cave, 30°49′25.9″ N, 50°25′37.9″ E, 812 m, 16.vi.2018, NBCL, Rahideh, S., & Muilwijk, J.	–	–	–	–
D. achaemenius sp. nov.	1 male, 1 female, paratypes, Iran, Kohgiluyeh Va Boyer Ahmad, Suq, Suq cave, 30°49′25.9″ N, 50°25′37.9″ E, 812 m, 16.vi.2018, CMU, Rahideh, S., & Muilwijk, J.	–	–	–	–
D. hetschkoi matilei	1 male, Iran, Kerman Jiroft, Narab, 900 m, 16.xi.1999, HMIM, Badii, Bar. Mof.	–	–	–	–
D. kileri	1 male, holotype, Iran, Kohgiluyeh Va Boyer Ahmad, Kiler cave, 31°17′96″, E 50°35′13″, 1610 m, 27.x.2011, N 31°17′96″, E 50°35′13″, 1610 m, ZM–CBSU. Malek-Hosseini, M.J.	–	–	–	–
D. kileri	1 males and 2 females, Iran, Kohgiluyeh Va Boyer Ahmad, Kiler cave, 31°17′96″, E 50°35′13″, 1610 m, 14.vi.2018, CMU, Rahideh, S., & Muilwijk, J.	–	–	–	–
D. kileri	1 male, 1 female, Iran: Kohgiluyeh Va Boyer Ahmad, Kiler cave, 31°17′96″, E 50°35′13″, 1610 m, 14.vi.2018, HMIM, Rahideh, S., & Muilwijk, J.	–	–	–	–
D. kileri	1 male, Iran, Kohgiluyeh Va Boyer Ahmad, Kiler cave, 31°17′96″, E 50°35′13″, 1610 m, 14.vi.2018, CMU, Rahideh, S., & Muilwijk, J.	MZ033183	MZ042532	MZ043110	MZ044285
D. koeni	1 male, Iran, Khuzestan, Pole-e Tang, 60 km NW Andimeshk, Loc. No. 284, 10–11.iv.1977, MNP, Muilwijk, J.	–	–	–	–
D. koeni	1 female, paratype, Iran, Khuzestan, Lake Izeh, 01.iv.2007, CMU. Muilwijk, J.	–	–	–	–
D. mohammadzadehi	1 male, holotype, Iran, Fars, Estahban, 25.iv.2006, 2380 m, MNP, Muilwijk, J.	–	–	–	–
D. mohammadzadehi	1 female, paratype, Iran, Fars, Estahban, 2380 m, 25.iv.2006, CMU. Muilwijk, J.	–	–	–	–
D. nezelensis sp. nov.	1 male, holotype, 1 female, paratype, Iran, Kohgiluyeh Va Boyer Ahmad, Nezel cave, 30°47′28.62″ N, 50°56′53.83″ E, 2307 m, 12.vi.2018, HMIM, Porebrahim, M., Azizi, S., Rozbehi, Z., Rahideh, S., & Muilwijk, J.	–	–	–	–
D. nezelensis sp. nov.	1 male, paratypes, Iran, Kohgiluyeh va Boyer Ahmad, Nezel cave, 30°47′28.62″ N, 50°56′53.83″ E, 2307 m, 15.xi.2016 / CMU, Malek-Hosseini, M. J.	MZ033192	MZ042534	MZ043721	MZ043751
D. nezelensis sp. nov.	2 males and 1 female, paratypes, Iran, Kohgiluyeh Va Boyer Ahmad, Nezel cave, 30°47′28.62″ N, 50°56′53.83″ E, 2307 m, 12.vi.2018, CMU, Porebrahim, M., Azizi, S., Rozbehi, Z., Rahideh, S., & Muilwijk, J.	–	–	–	–
D. nezelensis sp. nov.	1 femal,e paratype, Iran, Kohgiluyeh va Boyer Ahmad, Nezel cave, 30°47′28.62″ N, 50°56′53.83″ E, 2307 m, 9.x.2017, ZM–CBSU, Tahami, M. S.	–	–	–	–